

SOME CHARACTERISTICS OF THE USE OF THE ACOUSTIC EMISSION METHOD IN THE STUDY OF THE FRAGMENTATION OF SINGLE FIBERS IN A POLYMER MATRIX

Yu. A. Gorbatkina, Yu. G. Korabel'nikov,
V. P. Tamuzh, T. Yu. Zakharova,
I. A. Rashkovan, and A. A. Karklin'sh

The breakdown processes taking place in a reinforced single-fiber composite during its loading in the direction of the fiber axis have attracted the close attention of researchers in the last few years [1-7]. This is due to the fact that the study of the process of fiber fragmentation in such a model composite makes it possible to determine the so-called critical fiber length l_{cr} , a property that is of key importance for predicting the mechanical behavior of the composite. Knowing l_{cr} , one can estimate the shear adhesion strength of the fiber-matrix interface from the equation

$$\tau = \sigma_{cr} d/2l_{cr}, \quad (1)$$

where σ_{cr} is the fiber strength at the critical length and d is the fiber diameter. Many questions associated with the use of this equation are discussed in a review [8].

It was shown in [5-7] that in studying the process of fragmentation in a reinforced single-fiber composite, one can obtain from a single experiment the values of not only l_{cr} but also σ_{cr} , and the scale dependence of the strength of the fiber on its length l , i.e., the constants of the relation

$$\lg \sigma = A - B \lg l. \quad (2)$$

These data are also necessary for predicting the mechanical behavior of fiber-reinforced composites [9, 10].

The lengths of the fragments formed by the fragmentation can be measured directly under a microscope or calculated by recording the number of acoustic emission (AE) signals accompanying the fragmentation. Use of the AE method for recording breakdown events provides the opportunity for a broader study of breakdown processes than in optical microscopy, since it is thus possible to record not only the number of breakdown events, but also their energy. We should not only the number of breakdown events, but also their energy. We should also note that the AE method is not only more versatile (for example, it makes it possible to study the processes in opaque media), but also simpler than the optical method, which is described in [6]. However, the AE method is used to record all the breakdown events taking place in the specimen. Therefore, the problem arises of identifying the signals associated with different modes of breakdown of fiber, interface, matrix).

This paper proposes a new method of processing AE signals that permits a more reliable separation of the fiber fragmentation process from all other processes.

The measurements were carried out on specimens consisting of an ÉDT-10 epoxy matrix and UKN carbon fibers. The method of preparation of the specimens and the measurement procedure are described in [7]. In connection with the stated problem, three to four fiber-containing specimens and one to two specimens of the pure matrix were studied in each series of experiments. Figure 1 shows typical curves usually recorded in the AE study of fiber fragmentation processes. As expected, the introduction of a single fiber into the resin does not change the appearance of the σ vs ε curve but sharply increases the number of AE signals. This pattern, associated with the introduction of a carbon fiber into the epoxy matrix, had been observed earlier [1].

Chemical Physics Institute, Russian Academy of Sciences, Moscow. Institute of Polymer Mechanics, Latvian Academy of Sciences, Riga. UVIKOM TOO, Moscow Oblast. Translated from *Mekhanika Kompozitnykh Materialov*, No. 6, pp. 734-740, November-December, 1993. Original article submitted July 26, 1993.

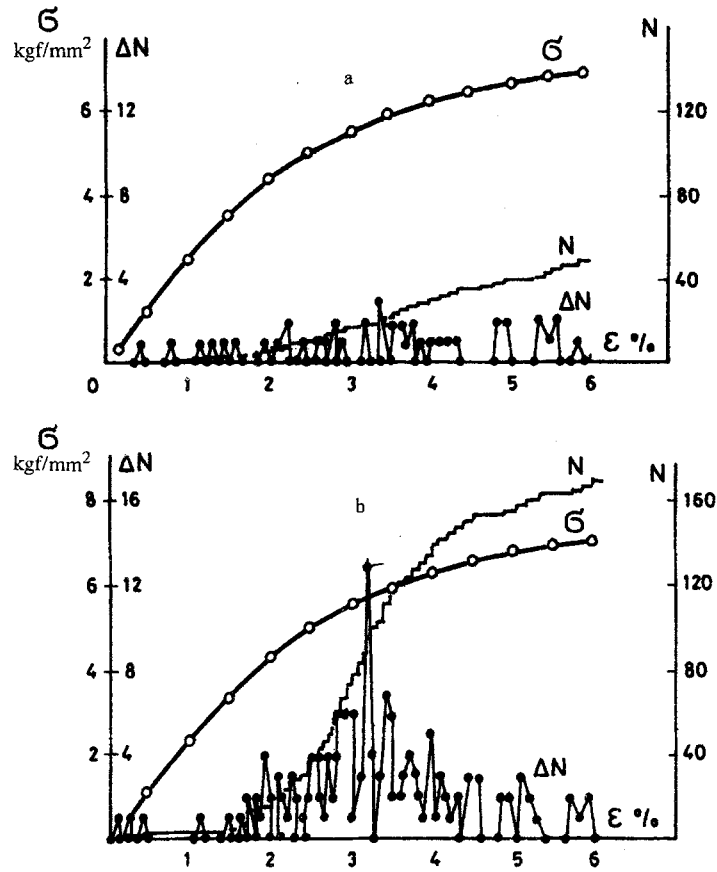


Fig. 1. Change in stress σ , in number of AE signals per unit time ΔN , and in total number of AE signals N in specimens of EDT-10 epoxy resin deformed without fiber (a) and reinforced with a single UKN carbon fiber (b).

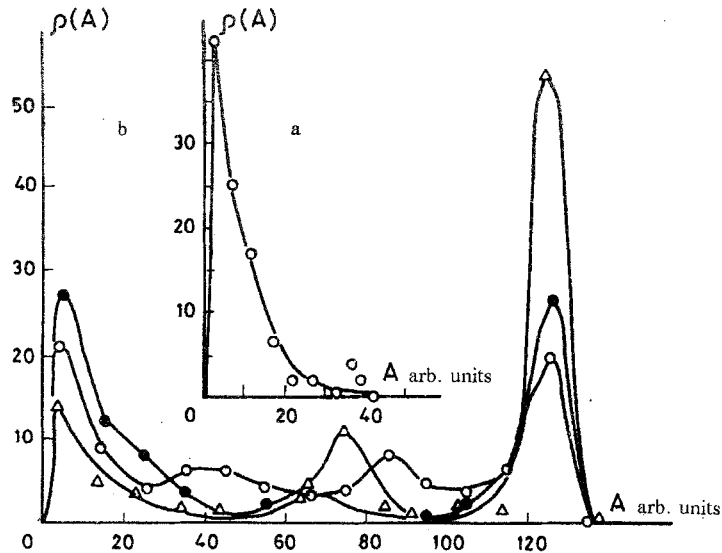


Fig. 2. Distribution of AE signal amplitudes in specimens of EDT-10 epoxy resin without fiber (a) and reinforced with a single UKN carbon fiber (b):

●) No. 1; ○) No. 2; △) No. 3.

In the presence of the fiber, there is not only an increase in the total number of signals, but also a change in the nature of their distribution with time and in their energy spectrum. This shows up clearly in the analysis of the amplitudes of incoming signals (Figs. 2 and 3).

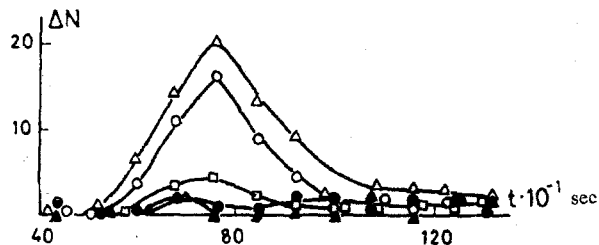


Fig. 3. Kinetics of appearance of signals with different amplitudes as the specimen is loaded: $A = 0-10$ (●); $10-20$ (▲); $70-80$ (□); $40-130$ (Δ); $120-130$ arb. units (○).

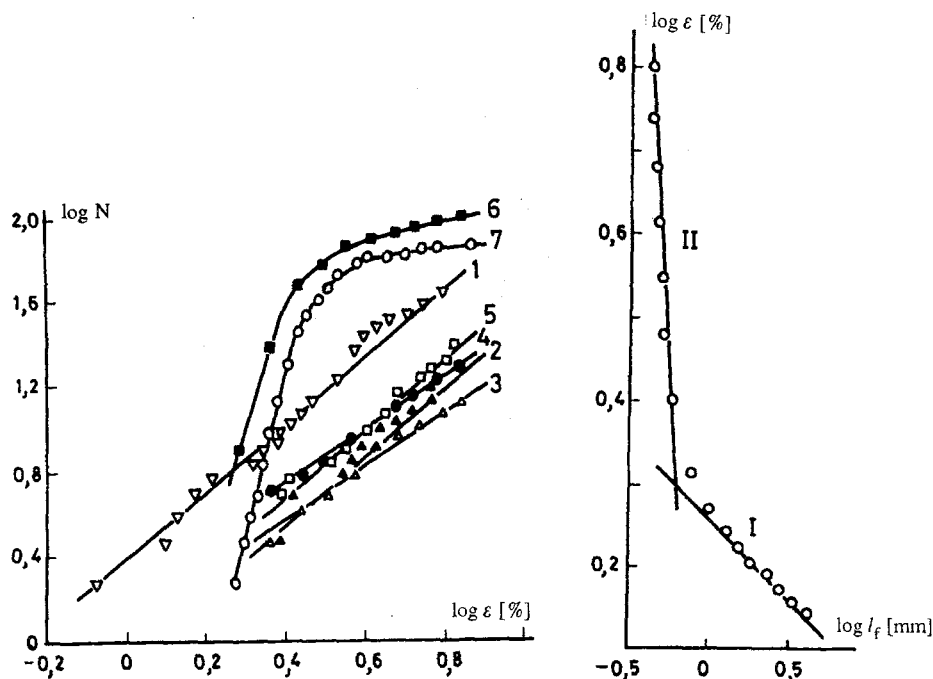


Fig. 4

Fig. 5

Fig. 4. Number of AE signals N vs strain ϵ in log-log coordinates for specimens of ÉDT-10 epoxy resin without fiber (1, 2) and reinforced with UKN single carbon fiber (3-7): $A < A_0^*$, $A_0^* = 10$ (3), 20 (4), 40 arb. units (5); $A = 0-130$ arb. units (6, all amplitudes); $A \geq A_0^* = 40$ arb. units (7).

Fig. 5. Strain ϵ vs fragment length l_f during loading of a specimen reinforced with a single UKN fiber.

For the nonreinforced matrix (see Fig. 2a), the amplitude distribution is unimodal, and the position of the maximum is stable: For all the specimens, it is observed at $A = 5-6$ arb. units. When the fiber is introduced (see Fig. 2b), the amplitude distribution is bimodal and polymodal. The position of the first and last maxima is stable: They are observed at $A = 5$ arb. units and $A = 125$ arb. units, respectively. The intermediate maxima do not have a constant position. However, the second maximum is observed with the highest probability at $A = 40-80$ arb. units. The height of the maxima varies from specimen to specimen for both the reinforced and nonreinforced resins. Each of the maxima of the $\rho(A)$ curve is naturally attributed to the presence in the specimens of defects of different degrees of risk at which the degradation takes place.

A comparison of the data of Fig. 2a and b suggests that signals with small amplitudes ($A < 40$ arb. units) are due to the breakdown of the matrix, and all the remaining signals are due to the breakdown of the fiber (and interface). This conclusion becomes more convincing later an analysis of the kinetics of arrival of signals with different amplitudes. It follows

TABLE 1

Range of amplitude A, arb. units	N_{max}	δ , mm	l_{cr} , mm		A	B
			$4/3\delta$	at the point of intersec- tion		
0...130	100	0,325	0,433	0,590	2,697	0,285
40...130	75	0,433	0,572	0,563	2,632	0,198

from the data of Fig. 3 that signals with amplitudes $A < 40$ arb. units during the breakdown of both the pure matrix and the fiber-reinforced matrix are almost uniformly distributed over time; their kinetics are not related to the magnitude of deformation of the loaded specimen.

In contrast to the signals of small amplitude, all other signals are clearly related to the magnitude of deformation of the specimen. They begin to show up at fairly high values of σ and ε (see Fig. 1). The number of breakdown events increases sharply in a narrow range of ε , and they practically cease after this range has been traversed. Such kinetics of signal arrival are completely consistent with the general interpretations of the processes taking place in specimens of this kind [1-8] (interpretations of fragmentation of carbon fibers after they have reached the breaking strains).

We can state that the kinetics of arrival of large-amplitude signals ($A_{av} \approx 125$ arb. units), corresponding to the last maximum, and signals with amplitudes ($A \approx 40-80$ arb. units), corresponding to an intermediate maximum, are practically the same. It is highly tempting to attribute the former signals to fiber fragmentation and the latter signals to the breakdown of the interface. However, the transition from this hypothesis to a reliable statement requires further studies.

As already noted, analysis of the signal arrival kinetics showed that the accumulation rate of signals formed during the breakdown of the matrix and fiber is not the same. This is reflected in Fig. 4. It is evident that as the matrix is deformed, the absolute number of signals for different specimens at different stages of deformation may prove different, but the rate of their arrival, i.e., the quantity $N' = d \log N / d \log \varepsilon$, remains practically constant for all the specimens, as was to be expected from the data of Fig. 3.

For the fiber-reinforced specimens, the $\log N$ vs $\log \varepsilon$ curves are clearly divided into two segments (see Fig. 4). Their slopes differ from those for the pure matrix. However, if the $\log N$ vs $\log \varepsilon$ curve is plotted for the reinforced specimens, small-amplitude signals being used, straight curves are obtained whose slope N' is very close to the slope of the corresponding straight curves for the nonreinforced specimens. This slope depends on the maximum amplitude A_0 of the signals due to the breakdown of the matrix. It is clear from the data of Fig. 4 how this slope changes with A_0 . It is also clear that at a certain value $A_0 = A_0^*$, the slopes of the straight curves for the reinforced and nonreinforced specimens practically coincide. This is observed when $A_0^* = 40$ arb. units, i.e., when the signals described by the first maximum of the $\rho(A)$ curve (see Fig. 2), and which we explain by the breakdown of the matrix, become exhausted. If the signals for which $A < A_0^*$ are neglected, the shape of the $\log N$ vs $\log \varepsilon$ curve remains unchanged: As before, the curve clearly shows two linear segments with slopes different from that of the straight $\log N$ vs $\log \varepsilon$ curve corresponding to the matrix (see Fig. 4). Thus, analysis of the amplitudes of the AE signals and of their arrival kinetics permits a reliable separation of signals due to the breakdown of the reinforcing element (and interface) from signals due to degradation of the matrix. This analysis also shows that the characteristics of the energy spectrum associated with the events of breakdown of the matrix and fibers present in the matrix are substantially different. We note that the conclusion that the rates of accumulation of signals originating from centers of different types of breakdown may prove significant for systems in which active breakdown of the fiber and matrix takes place practically at the same time, and signals from components undergoing breakdown become superimposed, for example, for systems with low-strength and low-modulus fibers. After finding the value of amplitude A_0^* , for each strain (stress) level one can determine the number of signals N^* with amplitudes greater than A_0^* . Curve 7 in Fig. 4 is just such a plot of N^* vs ε .

Knowing $N^* = N^*(\varepsilon)$, one can follow the change in average length l_{av} of the fragments into which the fiber breaks down as the specimen is deformed. Such a curve is shown in Fig. 5. When this curve was plotted, the value of l_{av} was calculated as $l_{av} = l_0 / (N^* + 1)$. The curve is clearly divided into two segments. Such division indicates different mechanisms of degradation. In segment I, the fiber breaks down into fragments of different lengths whose strength is higher than that of the initial fiber because of the existence of a scale dependence. As the load increases, the increase in stresses on the fragments and their further fragmentation continue until the matrix is able to transfer these stresses across the interface. Thus, the

location of the knee on the $\log \varepsilon$ vs $\log l_{av}$ curve corresponds to the value of strain (stress) at which shear failure takes place at the interface for certain fragments.

If all the fragments simultaneously reached the critical length l_{cr} , to which only one value of the fiber strength and adhesion strength of the fiber-matrix bond would correspond, the $\log \varepsilon - \log l_{av}$ curve in segment II would be a vertical straight line. The slope, different from 90° , of segment II is explained by the always-present spread of the value of the adhesion strength and strength of the fibers, and hence, by the spread of the values of the critical lengths. The average length of the fragments corresponding to the point of intersection of the straight lines in Fig. 5 may be treated as a quantity characterizing the adhesion strength and critical length of the given fiber-matrix pair. In the literature (see, for example, [8 and 10]), the calculation of l_{cr} sometimes involves the use of the limiting (minimum) value of the average length of the fragment $\delta = l_{av} = l_0 / (N_{max} + 1)$, and the value of the critical length is taken to be $l_{cr} = (4/3)\delta$. However, the asymptotic value of l_{cr} can only be obtained by testing specimens in which the fiber fragmentation ends before the specimen fails. This is not always observed. In the experiments, there are specimens in which the limiting value of l_{av} is not reached. At the same time, the knee of the $\log \varepsilon - \log l_{av}$ curve is observed for all the specimens. It was also found that the value of l_{av} corresponding to the knee point (see Fig. 5) is quite reproducible.

The l_{cr} values determined by both methods for the system in question are listed in Table 1. In the case under consideration, we found (without claiming generalization), and the l_{cr} values (if AE signals of small amplitude are neglected) determined by these methods were practically the same.

The $\log \varepsilon - \log l_{av}$ curve can be used for plotting the scale dependence of fiber strength, i.e., for determining the parameters A and B of Eq. (2). At the same time, it is necessary to allow for the fact that the true strain of the fiber in the specimen differs from the measured value ε . In [10], possible reasons for this difference are discussed, and a correction method is proposed. The plot in Fig. 5 takes this correction into account. Knowing the elastic modulus of the fiber (and assuming, as usual, that it is independent of the length), one can use the data of segment I in Fig. 5 to determine the fiber strength and plot the dependence (2) $\log \sigma - \log l$. The parameters of this dependence are also listed in Table 1.

Thus, analysis of the energy spectrum of AE signals and of the kinetics of arrival of different-amplitude signals permits a reliable separation of signals pertaining to different modes of failure. This increases the effectiveness of the use of the AE method for studying the process of fragmentation of a fiber located in a polymer matrix.

Conclusions. The energy spectra of acoustic signals during stretching of an epoxy specimen reinforced with carbon fiber and of a pure epoxy matrix differ substantially. Results of a comparison of these spectra make it possible to distinguish acoustic emission signals due to failure of the fiber during stretching of a reinforced composite and to plot curves of the average length of failing fiber fragments as a function of strain.

REFERENCES

1. N. Narisawa and H. Oba, "An evaluation of acoustic emission from fiber-reinforced composites," *J. Mater. Sci.*, **19**, 1777-1786 (1984).
2. W. D. Bascom and R. M. Jensen, "Stress transfer in single fiber/resin tensile tests," *J. Adhesion*, **19**, 219-239 (1986).
3. L. T. Drzal, M. I. Rich, and P. F. Loid, "Adhesion of graphite surface treatment," *J. Adhesion*, **16**, 1-30 (1982).
4. W. A. Fraser and J. H. Ancker, "Evaluation of surface treatment for fibers in composite materials," *J. Polymer Composites*, **4**, No. 4, 238-248 (1983).
5. USSR Authorship Certificate 1704015, "A method for determining the scale dependence of the strength of a fiber on its length," Yu. G. Korabel'nikov, I. A. Rashkovan, V. P. Tamuzh, A. A. Karklin'sh, Yu. A. Gorbatkina, and T. Yu. Zakharova, Applied for a September 8, 1991. *Otkrytiya Izobret.*, No. 1, 168-169 (1992).
6. H. D. Wagner and A. Eitan, "Interpretation of the fragmentation phenomenon in single-filament composite experiments," *Appl. Phys. Lett.*, **56**, No. 20, 1965-1967 (1990).
7. V. P. Tamuzh, Yu. G. Korabel'nikov, I. A. Rashkovan, A. A. Karklin'sh, Yu. A. Gorbatkina, and T. Yu. Zakharova, "Determination of the scale dependence of the strength of fibrous fillers and evaluation of their adhesion to the matrix, based on the result of tests of elementary filaments in a polymer block," *Mekh. Kompozitn. Mater.*, No. 4, 641-647 (1991).
8. S. F. Zhandarov, E. V. Pisanova, and V. A. Dovgyalo, "Fragmentation of a monofilament during stretching in a matrix as a method of determining adhesion," *Mekh. Kompozitn. Mater.*, No. 3, 384-403 (1992).

9. Yu. G. Korabel'nikov, O. F. Siluyanova, V. P. Tamuzh, A. N. Shiryaev, I. L. Kumok, and M. T. Azarova, "Basic patterns of manifestation of the mechanical properties of the filler in a unidirectional composite," *Mekh. Kompozitn. Mater.*, No. 2, 270-274 (1987).
10. Yu. G. Korabel'nikov, V. P. Tamuzh, O. F. Siluyanov, V. M. Bondarenko, and M. T. Azarova, "Scale effect of the strengths of fibers and properties of unidirectional composites based on them," *Mekh. Kompozitn. Mater.*, No. 2, 195-200 (1984).

METHODS OF FATIGUE PREDICTION FOR COMPOSITE LAMINATES.

A REVIEW

J. Andersons

A continuous change in the mechanical properties of composite materials caused by microdamage accumulation, redistribution of stresses due to the difference in the viscoelasticity and creep characteristics of the components, dissipative self-heating, etc., is observed during fatigue loading. As a critical level of damage is reached, the structure breaks down, i.e., it stops satisfying the imposed functional requirements. These requirements can be very different as a function of the area of application and responsibilities of the structure, but they usually include the residual strength, rigidity, and/or longevity of the composite material.

There are many studies of the behavior of composite materials under cyclic loading, and reviews are given in [1-3], for example. Because of the scientific interests of the investigators, special attention was focused on the stages and micro-mechanics of fatigue failure of heterogeneous materials in [1], a phenomenological description of damage accumulation and the correlation between the damages and the effective characteristics of the material in [2], and formulation of a fatigue theory in terms of residual strength and rigidity and statistical methods of selecting an adequate model in [3]. Each of these approaches undoubtedly has its own area of application, as well as its own limitations.

We attempted to compare the methods proposed in the scientific literature for predicting the fatigue characteristics of a laminated fiber composite for use in engineering calculations. It is useful to distinguish the proposed methods of calculation as a function of the structural level on which the material is modeled. For a laminated fiber composite, in addition to its representation as a homogeneous anisotropic material, models with the "resolution" of the structural level of the layer and fibers are also used. Such a classification reflects both the history of the development and the logic of the use of the methods of estimating fatigue life: the level of describing the structure of the material is determined by the accuracy with which the problem posed must be solved, the existence (or possibility of obtaining) the initial experimental data for the calculation, and naturally, the character of the process of fatigue failure of the material.

1. Neglecting the structure of a composite in considering it as a homogeneous material with certain effective characteristics eliminates the possibility of calculating the strength parameters (since they are determined by the structure of the composite and vary significantly as a function of the stacking scheme). With this approach, the problem becomes one of not calculating, but of recalculating the fatigue characteristics of the material from one loading regimen to the other, and it is necessary to perform tests directly with samples with the stacking scheme of interest in the given case for obtaining the initial data. The group of problems which can be solved in this way is relatively broad: estimation of the resistance to multicyclic loading with brief tests [2, 4-8], calculation of the residual strength [9-27] and rigidity [28-30], estimation of the scale effect [9, 31], consideration of the effect of the average cycle stress (asymmetry of loading) [24, 32], loading frequency [33], and control tests [9, 34, 35], calculation of resource in block programmed and random loading [9, 15, 17-20, 26, 36-43], and plotting of the strength area [44-48]. We will example the most developed ones in more detail.

Institute of Polymer Mechanics, Latvian Academy of Sciences, Riga. Translated from *Mekhanika Kompozitnykh Materialov*, No. 6, pp. 741-754, November-December, 1993. Original article submitted July 8, 1993.